Fish and Shellfish Immunology 86 (2019) 186–195

Contents lists available at ScienceDirect

Fish and Shellfish Immunology

journal homepage: www.elsevier.com/locate/fsi

Full length article

Towards a better understanding of allograft-induced stress response in the pearl oyster *Pinctada fucata martensii*: Insights from iTRAQ-based comparative proteomic analysis

Wei Wang, Qiannan Lei, Haiying Liang*, Junjun He

College of Fisheries, Guangdong Ocean University, Zhanjiang, Guangdong, PR China

ARTICLE INFO

Keywords:
Pearl oyster
Nucleus implantation
Stress adaptation
Proteomics
iTRAQ

ABSTRACT

Implantation of a spherical nucleus into a recipient oyster is a critical step in artificial pearl production. The implanted nucleus is known to trigger cellular stress responses at several levels, yet the molecular mechanism underpinning physiological adaptation of the pearl oysters to nucleus implantation is still poorly understood. In this study, we took advantage of the iTRAQ-based proteomics and LC-MS/MS approach to look into allograft induced gene regulation at the protein expression level in the pearl oyster *Pinctada fucata martensii*, across a period of 30 days following nucleus implantation. A wide variety of proteins, including a group of immune-related proteins such as E3 ubiquitin-ligase and heat shock proteins, exhibited differential expression in response to the surgical operation. Further comparisons between different sampling points revealed that GO terms including "translation" and "oxidation-reduction process" and KEGG pathways including "glycolysis/gluconeogenesis" and "pyruvate metabolism" were significantly enriched at several time points, indicating the important roles of these molecular events in the stress response of pearl oysters to nucleus implantation. In addition, considerable discrepancy between protein expression level and gene transcript abundancy was identified, as only a few genes showed at least 2-fold expression changes at both proteomic and transcriptomic levels. The result implies that post-transcriptional gene regulation for the key proteins may represent an important aspect of allograft-induced stress response in the pearl oysters. Taken together, the data obtained would contribute to a deeper understanding of the molecular mechanisms enabling stress adaptation of the pearl oysters in response to nucleus implantation.

1. Introduction

Artificial pearl production involves the implantation of a spherical shell bead (or nucleus) imbedded in mantle pieces into the visceral mass of a recipient oyster [1]. The implanted mantle tissue, or allograft, will develop into a pearl sac and pearl nacre will be secreted from the sac, giving rise to the formation of a pearl [2]. Upon the stimulation of foreign mantle pieces, the oyster can quickly mount responses of its immune system to accommodate the effects of the allograft [3]. However, if the immune system fails to respond in a timely and effectively manner, the implanted nucleus will be eradicated from the body, leading to failure of pearl production and sometimes death of the oysters [4,5]. Hence, understanding the molecular mechanisms underpinning immune tolerance of the pearl oysters to allograft is critical for improving the performance of pearl culture [6].

The pearl oyster, *Pinctada fucata martensii*, is one of the most important marine oysters cultured widely for the production of pearls [7]. Improvement in the techniques of oyster breeding, cultivation and nucleus insertion has helped to increase the success rate of pearl culture, but the quality of cultured pearls remains unpredictable and immunogenic rejection still represents a major problem in pearl culture [8,9]. The implanted mantle pieces are known to trigger cellular stress responses of the oysters, with differential regulations at several levels [6]. To date, the immune responses of *P. fucata martensii* to nucleus implantation have been studied from different angles [10–12]. The antibacterial capability of the hemolymph was found to decrease significantly following the surgical operation [9], and activities of metabolic enzymes such as superoxide dismutase, lysozyme and antimicrobial peptides declined sharply after nucleus implantation, partially contributing to the high mortality rate of the pearl oyster [9]. Individual genes such as *AIF-1* and *Galactin* have been identified as involved in the wound healing and immune tolerance of *P. fucata*

* Corresponding author.College of Fisheries, Guangdong Ocean University, Zhanjiang, Guangdong, PR China..
E-mail address: zjlianghy@126.com (H. Liang).

https://doi.org/10.1016/j.fsi.2018.11.044
Received 14 August 2018; Received in revised form 10 November 2018; Accepted 16 November 2018
Available online 17 November 2018

martensii [12,13], but a systematic understanding of the molecular basis underlying allograft induced stress response is still lacking [14,15].

In recent years, the application of high-throughput biotechnologies, including next generation sequencing (NGS)-based transcriptomic analysis and isobaric tags for relative and absolute quantitation (iTRAQ)-based proteomics, has provided unprecedented opportunities for studies on non-model organisms to identify molecular players involved in various physiological processes [3,16,17]. Previously, the short-term transcriptomic responses of the pearl oyster *P. fucata martensii* to allograft or xenograft have been examined using the RNA sequencing method, and a large number of genes potentially involved in immune tolerance of the pearl oyster has been identified [10,17]. In our previous study, the chronic gene expression changes at seven time points over a period of 60 days following nucleus implantation have been thoroughly investigated in the pearl oyster *P. fucata martensii* [3]. A variety of genes were found to show differential expression at different time points, including many immune-related genes such as toll-like receptor, lectin, scavenger receptor, and peroxidase [3]. In addition, genes related to two pathways, namely "cell adhesion molecules" and "primary immunodeficiency" were proposed to play crucial roles in the immune tolerance of the pearl oysters [3].

Despite the progress in our understanding of the molecular mechanism underlying the physiological adaptation of the pearl oysters following nucleus implantation, the key molecular players involved in allograft-induced stress tolerance still remain to be validated from different perspectives [9,17]. In the current study, we took advantage of the iTRAQ-based proteomics and LC-MS/MS approach to look into allograft induced gene regulation at the protein expression level in the pearl oyster *P. fucata martensii*. Protein quantification and characterization were performed for samples taken at 0 day, 10 days, 20 days and 30 days post nucleus implantation, and the dynamic protein expression changes as well as associated biological processes and gene pathways under regulation were examined.

2. Materials and methods

2.1. Nucleus implantation and sample collection

Animals used in the experiment were collected from the Dajing Pearl Culture Base in Xuwen, Zhanjiang, Guangdong Province. The oysters were cultured in natural seawater throughout the experiment and the nucleus insertion was performed *in situ*. 2-years-old oysters with a shell length about 6–8 cm were used for the experiment. The implantation operation was performed by an experienced technician according to methods in previous studies [3,10]. Before the nucleus implantation, hemolymph from six oysters was extracted as the control group using 1 mL syringes. Following nucleus insertion, samples of hemolymph were taken from another six oysters at each of the following time points: 10 days post implantation (dpi), 20 dpi, and 30 dpi. The hemolymph was centrifuged at 3500 r/min for 5 min and the precipitant at the bottom was separated to collect hemocytes. The hemocytes were first placed in liquid nitrogen and then stored at −80 °C. Hemocytes from three individuals were mixed as a sample, and two replicate samples were prepared for each time point.

2.2. Protein preparation

Each sample was grinded in liquid nitrogen and transferred to a 5-mL centrifuge tube. Then a 5-fold volume of lysis buffer (8 M urea, 1% Protease Inhibitor Cocktail) was added to each sample and three times of sonication on ice were performed using a high intensity ultrasonic processor. The supernatant was then collected by centrifugation at 12,000 g and 4 °C for 10 min, and the protein concentration was measured with BCA kit according to the manufacturer's instructions. Following that, the protein solution was treated with 5 mM dithiothreitol for 30 min at 56 °C and 11 mM iodoacetamide for 15 min at room temperature in the dark. Then, trypsin was added at 1:50 trypsin-to-protein mass ratio to digest overnight and 1:100 trypsin-to-protein mass ratio for another 4 h digestion. The digested peptides were purified by the method of high-performance liquid chromatography (HPLC).

2.3. iTRAQ labeling and SCX fractionation

Total protein (~100 μg) extracted from each sample was digested with Trypsin Gold (Promega, USA) with a protein-to-trypsin ratio of 30:1 at 37 °C overnight. The digested peptides were dried by vacuum centrifugation and further processed in 0.5 M TEAB. The iTRAQ reagent (Applied Biosystems) were first thawed and treated with isopropanol, and then mixed with the digested peptides. Samples taken from 0 dpi to 30 dpi were labeled with iTRAQ reagents 113–121. The labeled peptides were then pooled and dried by vacuum centrifugation. Then, the peptide mixture was purified using strong cation exchange chromatography (SCX), and separated with a LC-20AB HPLC Pump system (Shimadzu, Japan). The peptide mixture was first treated with 4 mL buffer A (containing 25 mM NaH_2PO4 in 25% CAN with a pH of 2.7) and then loaded onto an Ultremex SCX column containing 5 mm particles (Phenomenex). The peptides were further eluted with buffer A and buffer B (comprising 25 mM NaH_2PO4 and 1 M KCl in 25% CAN with a pH of 2.7). By measuring the absorbance at 214 nm, elution was monitored, and fractions were collected every 1 min. The eluted peptides were pooled into 20 fractions, processed with a Strata X C18 column (Phenomenex) and vacuum-dried.

2.4. LC-MS/MS analysis

A Triple TOF 5600 System was utilized for LC- MS/MS analysis. Parameters used for the system included an ion spray voltage of 2.5 kV, curtain gas of 30 psi, nebulizer gas of 15 psi, and an interface heater temperature of 150 °C. MS operation was conducted using a RP of no less than 30,000 FWHM. Survey scans were acquired in 250 ms for IDA, and if a threshold of 120 counts per second (counts/s) was exceeded, up to 30 ion scans were collected. A multichannel TDC detector containing a four-anode channel was used to detect and sum ions from each scan at a 11 kHz pulse frequency. iTRAQ adjusted rolling collision energy and sweeping collision energy with 35 ± 5 eV were combined for application to all precursors. Peptides with +2 to +3 charge states were selected, and a fragment intensity multiplier value of 20 and a maximum accumulation time of 2*s* were applied.

2.5. Data analysis

The ProteinPilot Software v4.5 (SCIEX, USA) was used to analyze the original MS/MS data. For protein identification, the previously available transciptome annotation of *P. fucata martensii* was used as references. The Proteomics System Performance Evaluation Pipeline (PSPEP) in ProteinPilot was applied for false discovery rate (FDR) estimation. Only proteins with at least one unique peptide and an unused value above 1.3 were used for downstream analysis. As in other similar studies [18,19], peptides that met at least one of the following criterion were excluded from further analysis: (1) peaks of iTRAQ labels were not detected; (2) peptides were identified with low confidence; (3) peptides assigned to more than one protein; (4) the signal-to-noise (S/N) ratio was too low; (5) peptides with a combined feature probability < 30%. All MS/MS data were processed with the ProteinPilot software and protein abundance values were normalized before calculation of expression change ratios. A 2-fold difference and P-value < 0.05 were used as thresholds for significant differential expression. In addition, functional annotations of the proteins were conducted using Blast2GO program against the non-redundant protein database (NR; NCBI). The KEGG database (http://www.genome.jp/kegg/) were also used to identify significantly enriched pathways represented by the

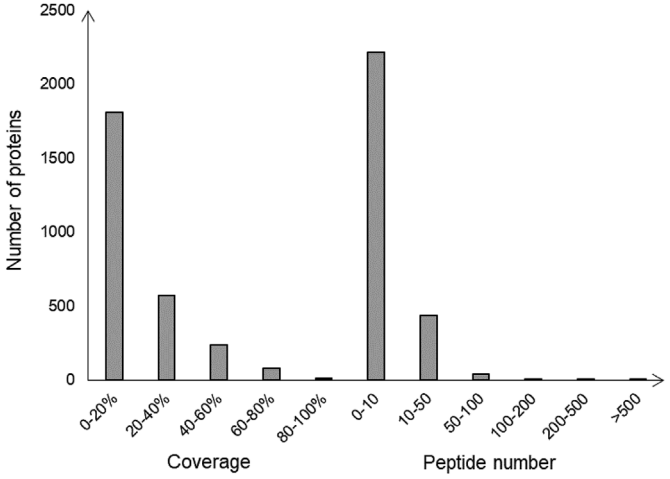

Fig. 1. Distribution of protein coverage (the left five columns) and the number of peptides matched to each protein (the six columns on the right).

differentially expressed proteins. Result from our previous transcriptomic study on the same group of samples was used to perform a comparison with data of the current study, and the online tool Morpheus (https://software.broadinstitute.org/morpheus/) was used to draw heatmaps summarizing genes that show consistent expression profiles at both transciptomic and proteomic levels.

3. Result

3.1. Identification of proteins

A total of 276,921 spectrums were obtained from the iTRAQ LC-MS/MS proteomic analysis. After elimination of labeling free and low-scoring spectra, the remaining spectrums were matched to 24,142 distinct peptides using a global FDR rate of 5%. These peptides were further mapped to 2705 proteins based on available transcriptome data of *P. fucata martensii*. The distribution of protein coverage and number of peptides matched to each protein were summarized in Fig. 1. As shown in the figure, a large number of the identified proteins (1,810) had a coverage below 20% and 2216 proteins had less than 10 peptides matched to them.

3.2. Quantitative proteomic analysis

In this study, differentially expressed proteins between adjacent sampling points (0 dpi vs 10 dpi, 10 dpi vs 20 dpi, and 20 dpi vs 30 dpi) were analyzed (Table S1). For each protein, a fold change of expression level over 2 was considered as up-regulation while a fold change less than 0.5 was considered as down-regulation. Using this criteria, the up-regulated and down-regulated proteins between each pair of samples were identified, and functional enrichment of GO terms and KEGG pathways associated with the differentially expressed proteins were also examined.

3.2.1. 0 dpi vs 10 dpi

A total of 319 proteins were detected as showing significant differential expression. Among them, 117 proteins were induced while

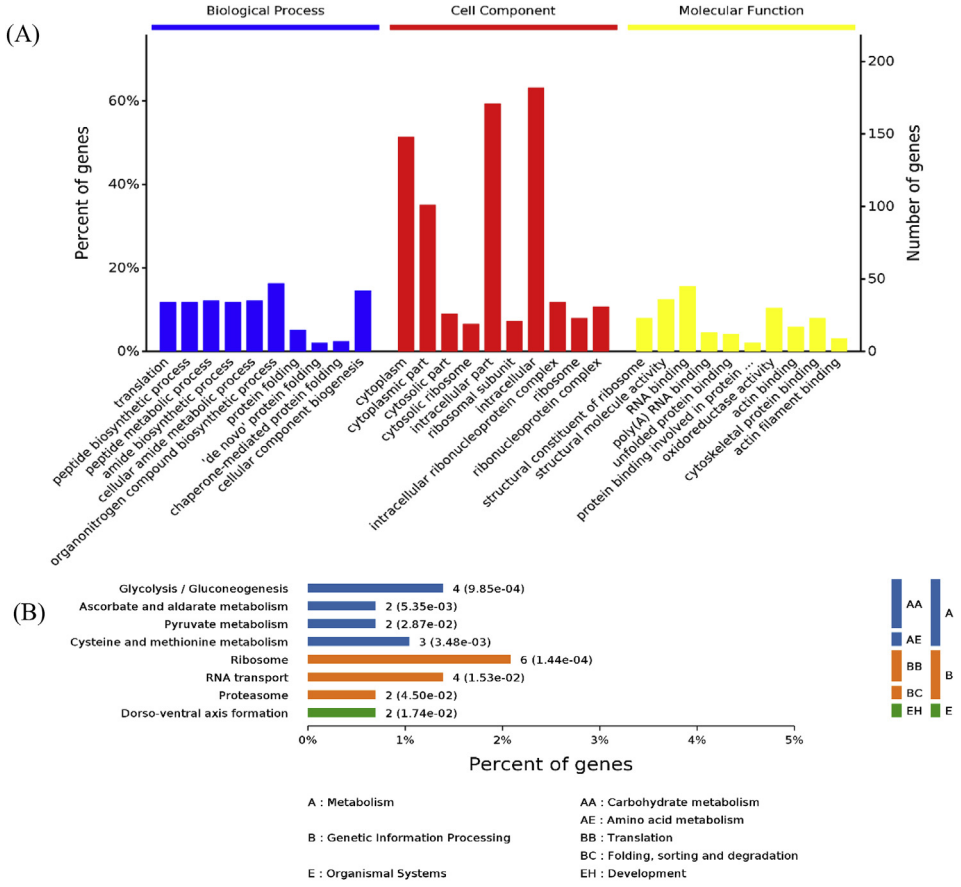

Fig. 2. Enrichment of Gene Ontology terms (A) and KEGG pathways (B) for differentially expressed proteins between 0 dpi and 10 dpi samples. The top GO terms in the category of biological process, cell component and molecular function as well as the most enriched KEGG pathways were shown.

202 proteins were repressed. Proteins showing the largest increase in expression levels included many proteins related to metabolism, such as 17-beta-hydroxysteroid dehydrogenase 14, serine threonine kinase 39, V-type proton ATPase subunit D, and arginine kinase. The most down-regulated proteins included ribosomal protein S5, leucine-zipper-like transcriptional regulator 1, antibacterial L-amino acid oxidase, fibroblast growth factor receptor 2, and heat shock protein HSP 90-alpha 1. To gain an overview of the physiological processes associated with these differentially expressed proteins, GO and KEGG enrichment analysis was further performed. The result showed that translation, peptide biosynthetic process and peptide metabolic process were the three most over-represented terms in the category of biological process, while structural constituent of ribosome, structural molecule activity and RNA binding were the three most over-represented terms in the category of molecular function (Fig. 2A). In terms of KEGG pathway enrichment, glycolysis, ascorbate and aldarate metabolism, pyruvate metabolism, cysteine and methionine metabolism, ribosome, RNA transport, proteasome, and dorso-ventral axis formation pathways were significantly enriched (Fig. 2B).

3.2.2. 10 dpi vs 20 dpi

Using the above mentioned criteria, 167 proteins were detected as showing significant differential expression between samples taken at 10 dpi and 20 dpi. Among them, 83 proteins were significantly induced while 84 proteins were significantly repressed. Proteins showing the largest magnitude of induction included nuclear ribonucleoprotein K, stromal membrane-associated protein 2, alpha-aminoadipic semialdehyde synthase, far upstream element-binding protein 3, and lysozyme. The most down-regulated proteins included extended synaptotagmin-like protein 2, adenylate kinase isoenzyme 1, arginine kinase, vitellogenin-6, protocadherin Fat 4, and monocarboxylate transporter 12. Following the identification of these differentially expressed proteins, GO and KEGG enrichment analysis was further conducted. The result showed that oxidation-reduction process, single-organism intracellular transport and single-organism metabolic process were the three most enriched terms in the category of biological process, while RNA binding, poly(A) RNA binding and oxidoreductase activity were detected as the three most enriched terms in the category of molecular function (Fig. 3A). In terms of KEGG pathway enrichment, glycolysis, pyruvate metabolism, glycerolipid metabolism, cysteine and methionine metabolism, and spliceosome pathways were significantly enriched (Fig. 3B).

3.2.3. 20 dpi vs 30 dpi

Between samples taken at 20 dpi and 30 dpi, a total of 173 proteins exhibited significant differential expression. 80 proteins displayed significant increase in expression levels while 93 proteins were significantly repressed. Proteins with the maximum levels of increase in expression included thymosin beta-4-like, tripartite motif-containing protein 2, transketolase-like protein 2, transmembrane protein C9orf5, and thioredoxin. In addition, the most down-regulated proteins included interferon-induced protein 44-like protein, bile acyl-CoA synthetase, Ras-related C3 botulinum toxin substrate 1, alpha-actinin, multimerin-1, and prostaglandin E synthase 3. GO and KEGG enrichment analysis was further conducted for these differentially expressed proteins. The result revealed that amide biosynthetic process, organonitrogen compound biosynthetic process, peptide biosynthetic process were the three most enriched terms in the category of biological process, while oxidoreductase activity, structural constituent of ribosome, and structural molecule activity were detected as the three most enriched terms in the category of molecular function (Fig. 4A). In terms of KEGG pathway, synthesis and degradation of ketone, cysteine and methionine metabolism, and taurine and hypotaurine metabolism were significantly enriched (Fig. 4B).

3.2.4. Gene network and protein interaction analysis

To examine the changing profiles of differentially expressed proteins from a comparative and dynamic point of view, analysis of protein-protein interactions for each pair of samples was further conducted, and the enriched GO terms or KEGG pathways associated with these interacting proteins were also identified. As shown in Fig. 5, the profiles of protein interactions for the first two groups (0 vs 10 dpi and 10 vs 20 dpi) were quite similar. Although proteins present in the network varied between the two groups, their associated GO terms or KEGG pathways shared much similarity. Both these groups contained ascorbate and aldarate metabolism, glycerolipid metabolism, glycolysis/gluconeogenesis, pyruvate metabolism, cysteine and methionine metabolism, and ribosome. By contrast, proteins present in the network for the group 20 vs 30 dpi were obviously distinct from the previous two groups, and most of their associated GO terms or KEGG pathways were only detected in this group (Fig. 5). These included the citrate cycle (TCA cycle), biosynthesis of unsaturated fatty acids, synthesis and degradation of ketone bodies, 2-oxocarboxylic acid metabolism, butanoate metabolism, taurine and hypotaurine metabolism, and mismatch repair.

3.3. Correlation between proteomic and transcriptomic analyses

Result of the proteomic analysis was compared with that of our previous transcriptomic study [3], and the correlation between the differentially expressed proteins and gene transcripts identified in the two studies were examined. Out of the 319, 167, and 173 differentially expressed proteins in the above three groups of comparison (Fig. 6), only 144, 62, and 77 corresponding genes showed consistent expression changes at the transcriptional level (Fig. 7 and Fig. 8).

Between 0 dpi and 10 dpi, 48 genes displayed increased expression levels in both proteomic and transcriptomic analyses, including cytochrome P450 3A29, pyruvate kinase, malate dehydrogenase, and syntaxin-7 (Fig. 7). Meanwhile, 96 genes showed reduced expression levels in both proteomic and transcriptomic analyses, including many ribosomal process related genes such as 60S ribosomal protein L38, 60S ribosomal protein L5, and ribosomal protein L14, and some well-characterized genes such as insulin-like growth factor 2 mRNA-binding protein 1, elongation factor 1 alpha, importin subunit alpha-7, receptor for activated C-kinase, and toll-like receptor 3 (Fig. 8).

Between 10 dpi and 20 dpi, 22 genes showing increased expression levels and 40 genes showing decreased expression levels in both proteomic and transcriptomic analyses were identified (Figs. 7 and 8). The up-regulated genes included synapse-associated protein 1, elongation factor 1 alpha, and histone h1-delta, while the down-regulated genes included peroxiredoxin-5, malate dehydrogenase, stress response protein NhaX and cytochrome p450 2C8.

Between 20 dpi and 30 dpi, 33 genes were detected as showing increased expression levels while 44 genes showed decreased expression levels (Figs. 7 and 8), in both proteomic and transcriptomic analyses. The up-regulated genes included actin-interacting protein 1, aldehyde oxidase, eukaryotic translation initiation factor 3 subunit b, and the down-regulated genes included G-protein-signaling modulator 2, tropomyosin and glyoxylate reductase.

In addition, when using the same criteria of a fold change value larger than 2 or less than 0.5 to define significant differential expression, only a handful of genes could be regarded as differentially expressed in both proteomic and transcriptomic analyses. The up-regulated genes with more than 2-fold increase in expression level in both analyses included Rab-18-B, syntaxin, histone h1-delta, myosin chain b, eukaryotic translation initiation factor 3 subunit b, extended synaptotagmin-like protein 2, and myotubularin-related protein 15 (MTMR15). Moreover, the down-regulated genes with more than 2-fold decrease in expression level in both analyses included spectrin beta chain, calponin-2, myosin heavy chain, sortilin, actin-binding Rho-activating protein-like, Elks/rab6-interacting protein, and several hypothetic proteins

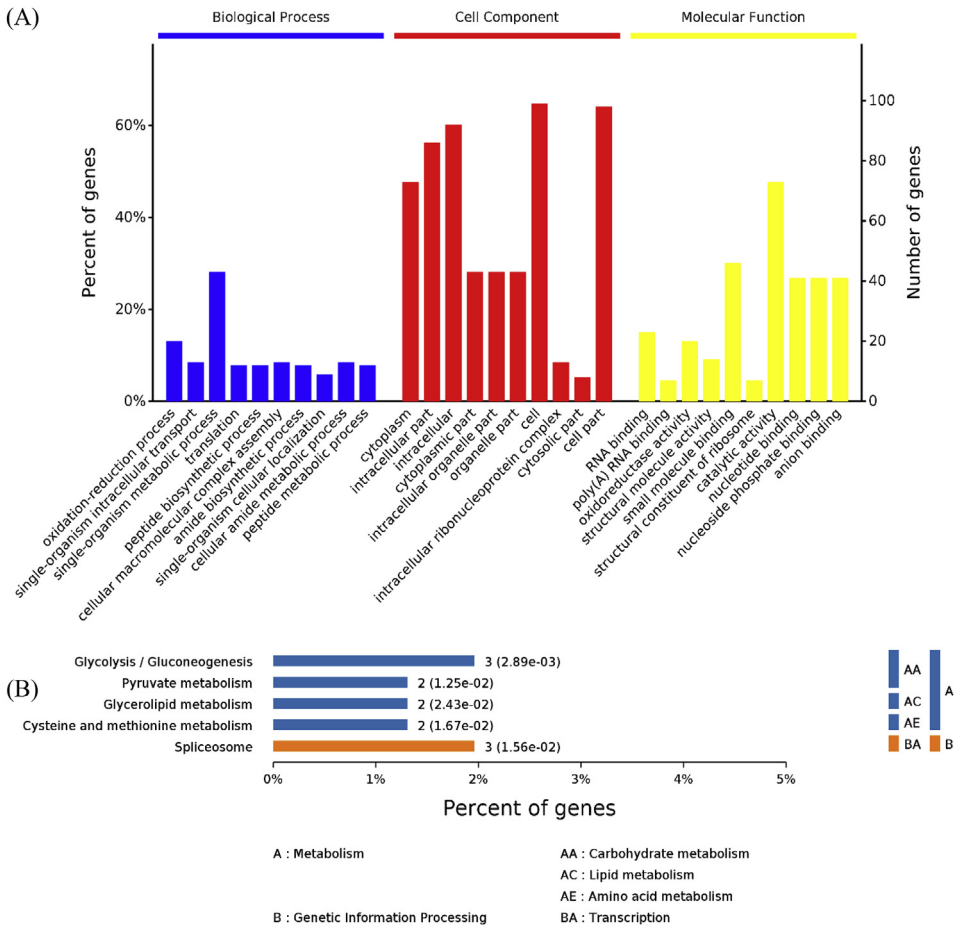

Fig. 3. Enrichment of Gene Ontology terms (A) and KEGG pathways (B) for differentially expressed proteins between 10 dpi and 20 dpi samples. The top GO terms in the category of biological process, cell component and molecular function as well as the most enriched KEGG pathways were shown.

with ambiguous annotation.

4. Discussion

P. fucata martensii is one of the most important marine shellfish for artificial pearl production in China [20]. As a key technique for artificial pearl culture, the operation of nucleus implantation has a major impact on the physiology of the pearl oyster and to a large extent determine the success of pearl culture [21]. Thus, the stress response and adaptation mechanism of pearl oysters to nucleus implantation has attracted wide attention from scholars and practitioners in the pearl culture industry [22–24]. Previously, to clarify the molecular mechanism underlying immune tolerance of *P. fucata martensii*, our research team performed a comprehensive transcriptomic study on the pearl oyster [3]. The chronic gene expression changes across a period of 60 days following nucleus implantation has been examined, and a variety of genes including many immune-related genes such as toll-like receptor and lectin were found to show differential expression at different time points [3]. Despite the progress that have been achieved, transcriptomic profiling may only provide clues on gene expression changes at the transcriptional level, and may offer limited insights into the physiological adaptation of pearl oysters in response to nucleus implantation [17].

In this study, iTRAQ technology was utilized to examine differentially expressed proteins during a period of 30 days following implantation of the nucleus, so as to identify candidate proteins and their associated molecular processes involved in the physiological adaptation of pearl oyster to nucleus implantation. Through comparison of protein expression profiles between the four sampling points, differentially expressed proteins with a wide range of biological functions were identified. Among them were a group of immune-related proteins, such as E3 ubiquitin-ligase, heat shock proteins (HSP), tumor necrosis factor receptor-associated factors (TRAF) and protocadherin (PCDH).

E3 ubiquitin-ligase is the main component of ubiquitin-proteasome degradation system [25]. Many research has shown that E3 ubiquitin ligase plays an important role in innate immunity [26]. Knockdown of E3 ubiquitin ligase gene in pDC cells resulted in inhibition of the TLR2/4/7/9 signaling pathways and impaired the immune defense response [27]. As a kind of E3 ubiquitin-ligase, tripartite motif (TRIM) protein is composed of RING finger, B-box and coiled-coil domains, and involved in important life processes such as cell cycle regulation, apoptosis, signal transduction, and antiviral response [28–30]. Previous studies reported that more than half of the 75 E3 ubiquitin ligases identified in mammalian cells were induced upon pathogenic stimulus [31], and about 20 homologues of E3 ubiquitin ligases were highly up-regulated in HEK293 cells to prohibit the multiplication and release of HIV or MLV [32]. In this study, it was found that expression of an E3 ubiquitin-ligase decreased gradually following nucleus implantation, and reached the lowest level on the 30th day. Moreover, two TRIM proteins also showed decreasing expression levels after nucleus implantation. It was thus speculated that the immune defense reaction of the oyster caused by the implantation of nuclear beads had weakened after 10 days, and the decreased expression of E3 ubiquitin-ligases may be necessary to inhibit the production of inflammatory reaction factors [31].

Heat shock proteins are a group of molecular chaperone proteins involved in protein folding and damage repair, and they are rapidly synthesized in the cell under stressful conditions [33]. HSP70 is one of the most conservative and abundant type in the HSP family [34]. Some

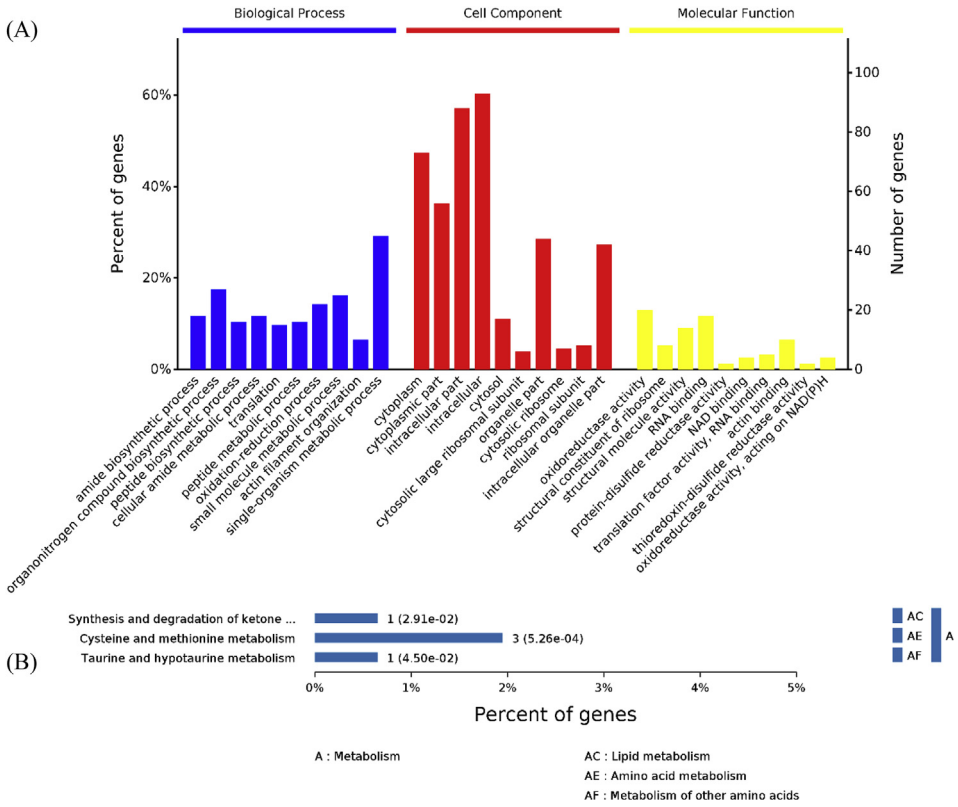

Fig. 4. Enrichment of Gene Ontology terms (A) and KEGG pathways (B) for differentially expressed proteins between 20 dpi and 30 dpi samples. The top GO terms in the category of biological process, cell component and molecular function as well as the most enriched KEGG pathways were shown.

studies have shown that HSP70 is involved in immune response and can inhibit inflammatory reaction [34]. It can inhibit the expression of inflammatory mediators such as interleukin-1 and tumor necrosis factor [35], and assist the immune defense system to identify and remove foreign invasive material [34], contributing to the activation of specific and non-specific immune responses [36]. In our study, expression of HSP70 was found to be significantly decreased on the 10th day, and then gradually increased but was still lower than the pre-implantation level on the 30th day. Repression of HSP70 may suggest that the cellular stress response machinery was affected by the immune defense system following nucleus implantation.

Tumor necrosis factor receptor-associated factors (TRAF) is a kind of joint protein implicated in signal transduction processes mediated by tumor necrosis factor receptors, toll and interleukin 1 receptors [37]. They are involved in a variety of biological processes including innate immune response, embryonic development, stress response and bone metabolism [38–40]. Some studies have shown that the RING region of TRAF2 and TRAF6 has the activity of E3 ubiquitin-ligase, and can activate downstream MAP3K family kinases such as MEK1-3 and NIK [37,41,42]. In the current study, a TRAF related protein was significantly up-regulated on the 10th day but then reduced to the control level on the 20th and 30th days following nucleus implantation. The result indicated that the TRAF protein was likely to participate in the immune regulation process of the pearl oyster, but its specific functional mechanism still needs further investigation.

PCDHs are a large family of cell adhesion molecules [43]. Studies on vertebrates have found that PCDHs were mainly expressed in the nervous system and were widely involved in intracellular signal transduction and intercellular adhesion [44]. Recent studies on PCDH family members have shown that PCDHs also participate in the negative regulation of cancer cell proliferation, migration and invasion [45,46]. In this study, 6 PCDHs were found to reach the maximum expression levels on the 20th day and gradually drop to the control level by the 30th day. Previous studies on *P. fucata martensii* reported that from 15 to 20 days after nuclear implantation, the outer epidermal cells of the mantle pieces would migrate to the surface of the pearl nucleus, giving rise to a stable pearl sac [8]. The induction of PCDHs on the 20th day after nuclear implantation implies that they are probably involved in the migration process of epidermal cells during pearl formation.

Other than the above mentioned immune-related proteins, GO functional enrichment analysis revealed that in the category of biological process, the “translation” process was significantly enriched throughout the whole experiment, and “oxidation-reduction process” was significantly enriched on the 20th and 30th day. Moreover, in the category of molecular function, the “RNA binding” and “oxidoreductase activity” terms were significantly enriched in all three groups of comparisons. Enrichment of these GO terms implies the important roles of these molecular events in the adaptation of pearl oysters to allograft [10]. In addition, “glycolysis/gluconeogenesis” and “pyruvate metabolism” pathways were significantly enriched in the first 20 days after nucleus implantation but were absent in the comparison between the last two time points, indicating the involvement of these pathways during the initial period of stress adaptation in response to allograft caused injury [3]. When protein-protein interactions for different groups of comparisons were further analyzed, it was noticed that GO terms or KEGG pathways associated with the interacting proteins were quite similar for the first two groups, 0 vs 10 dpi and 10 vs 20 dpi (Fig. 5). But the scenario for the last group (20 vs 30 dpi) was apparently distinct from the previous two groups, as the majority of the associated GO terms or KEGG pathways were unique for this group, implying that this period may require special cellular reprogramming to facilitate pearl formation and immune adaptation [3,47].

By comparing result of the current proteomic study and result of our previous transcriptomic study on the same samples, considerable discrepancy between protein expression data and gene transcript abundancy was noticed. A total of 319, 167, and 173 differentially expressed

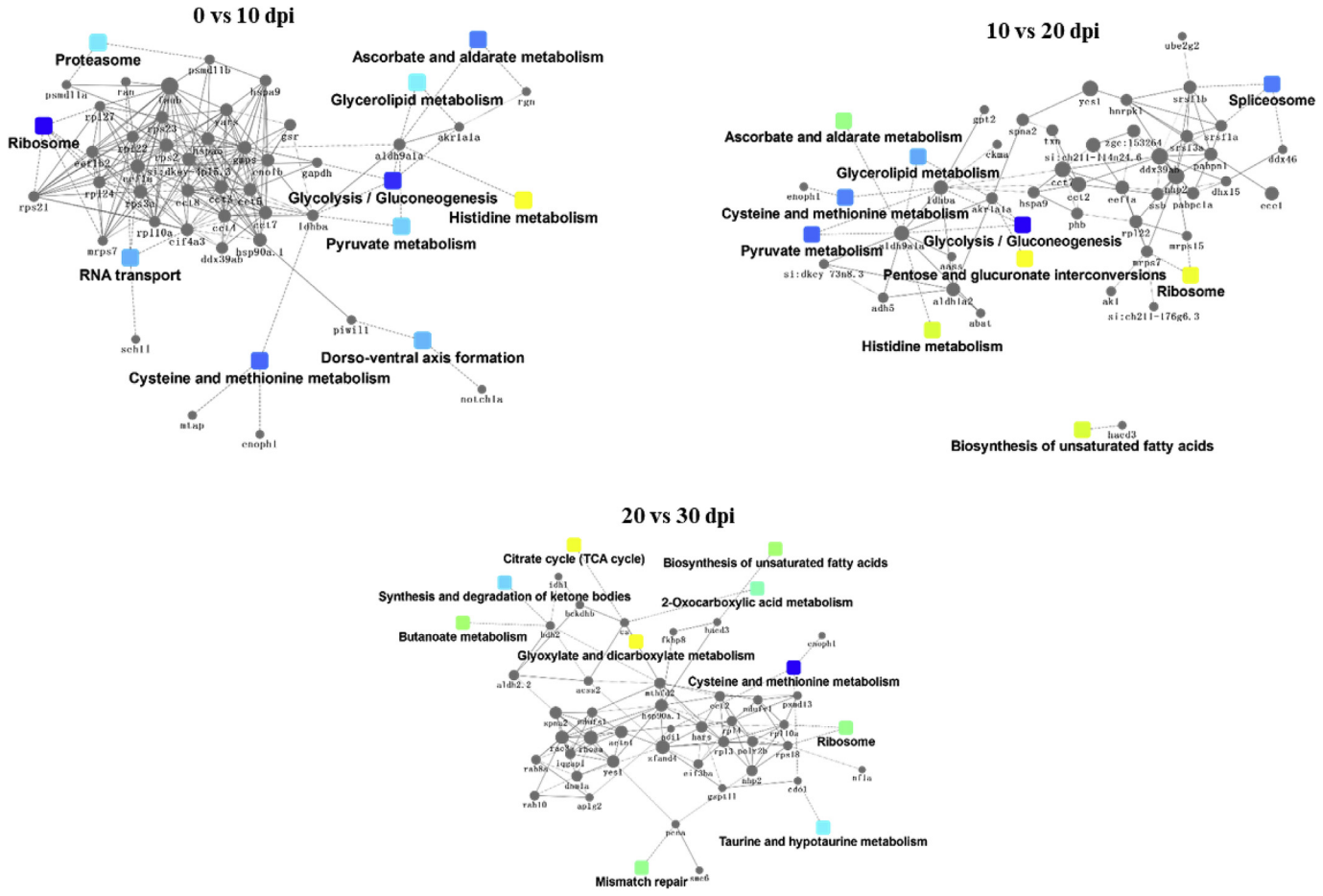

Fig. 5. Analysis of protein interactions for differentially expressed proteins between each pair of samples. The enriched GO terms or KEGG pathways associated with these interacting proteins were highlighted with different colors. The filled circles represent proteins and the filled boxes denote GO terms or KEGG pathways. (For interpretation of the references to color in this figure legend, the reader is referred to the Web version of this article.)

proteins were identified from the comparisons of 0 dpi vs. 10 dpi, 10 dpi vs. 20 dpi, and 20 dpi vs. 30 dpi, respectively (Table S1 and Fig. 6). However, only 144, 62, and 77 corresponding genes showed consistent expression changes (up-regulated or down-regulated in both analyses) on the transcriptional level. If the magnitude of expression change was taken into account, the number of genes showing accordant transcriptomic and proteomic changes was even less because very few transcripts also showed a fold change of expression level larger than 2

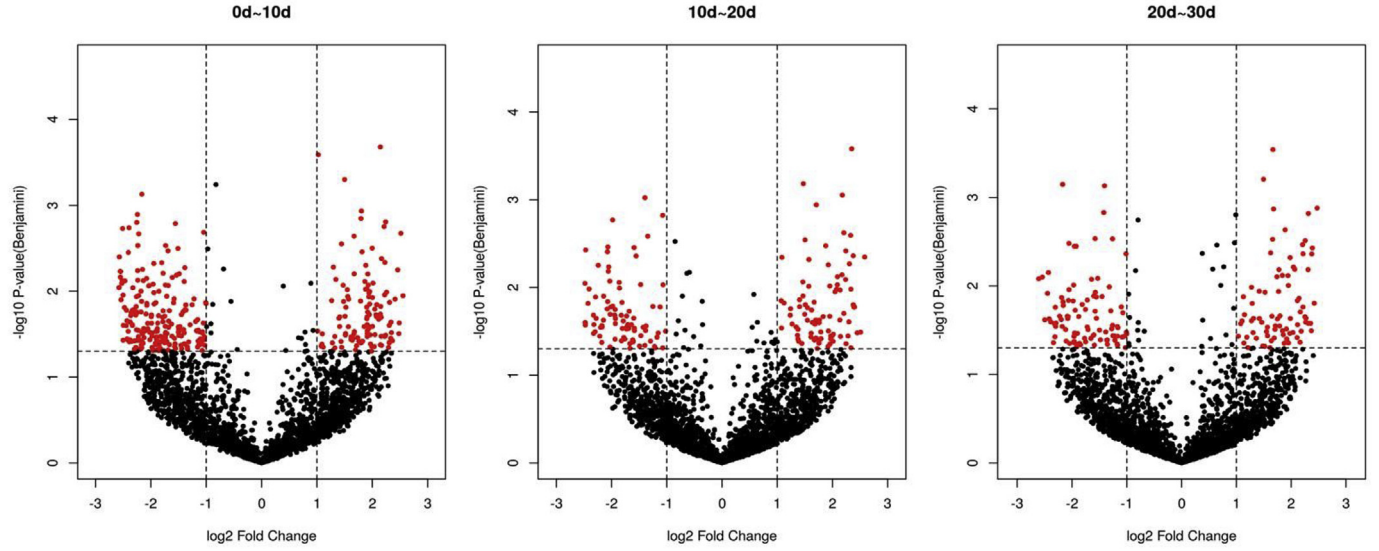

Fig. 6. Distribution of up- and down-regulated proteins and their P values. The horizontal and vertical axis represents log_2Fold-change and log_{10}P-value, respectively. The reds dots denote proteins with more than 2-fold expression changes and P values below 0.05.

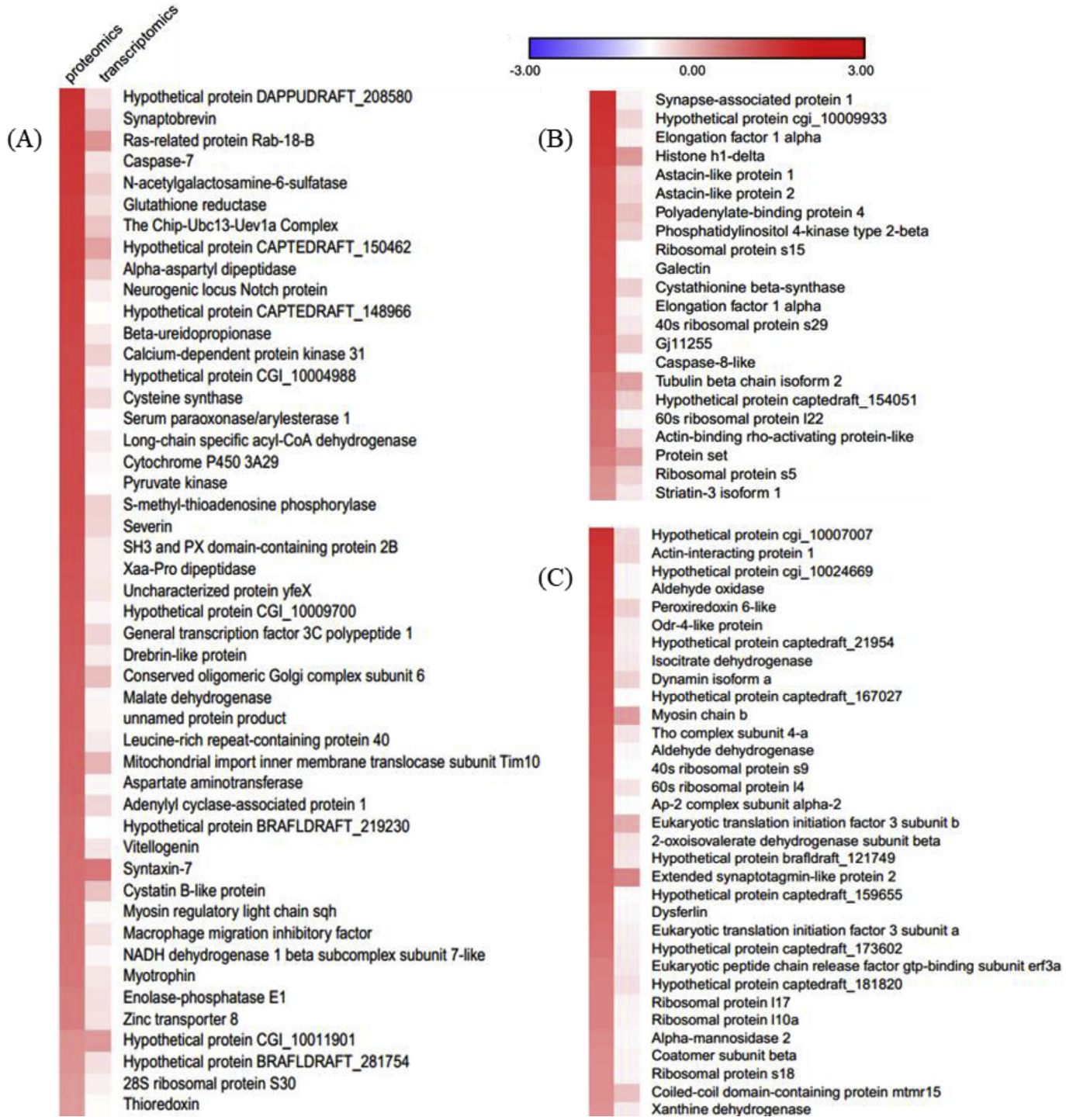

Fig. 7. Comparison of up-regulated genes between proteomic and transcriptomic analysis. (A) 0 dpi vs 10 dpi; (B) 10 dpi vs 20 dpi; (C) 20 dpi vs 30 dpi. Color bar showed different values of $\log_2$fold-change. In each group of comparison, the left column represented proteomics result while the right column represented transcriptomics result. (For interpretation of the references to color in this figure legend, the reader is referred to the Web version of this article.)

or less than 0.5. The up-regulated genes showing more than 2-fold increase in expression level in both proteomic and transcriptomic analyses, such as Rab-18-B, syntaxin and histone h1-delta, and the down-regulated genes with more than 2-fold decrease in expression level in both analyses, such as spectrin beta chain, calponin-2 and Sortilin, may represent attractive targets that can be explored in following in-depth functional studies. They may also be developed as molecular markers for the application in pearl culture, as the expression profiles of these genes are likely to be associated with stress tolerance capacity or other quality traits of the pearl oysters [3,48,49]. In addition, the discrepancy between protein expression level and gene transcript abundancy further demonstrates that transcriptomic changes not necessarily translate into protein expression changes [50,51]. Post-transcriptional gene regulation, especially for the key proteins with potential pivotal roles in the physiological adaption to nucleus implantation, may represent an important aspect of allograft-induced stress response in the pearl oysters [52], which merits further finer-scale mechanistic studies in the future.

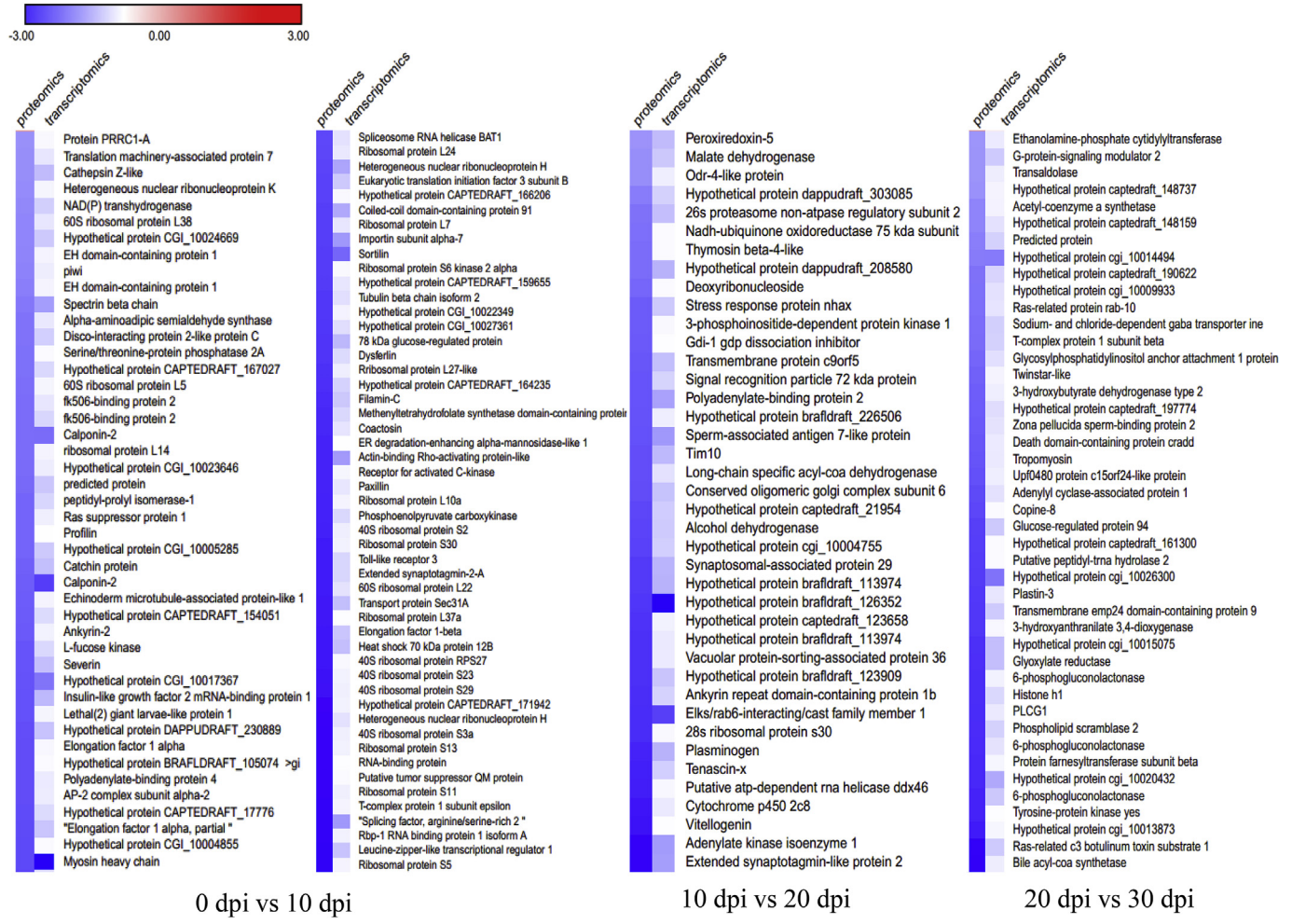

Fig. 8. Comparison of down-regulated genes between proteomic and transcriptomic analysis. Color bar showed different values of $\log_2$fold-change. In each group of comparison, the left column represented proteomics result while the right column represented transcriptomics result. (For interpretation of the references to color in this figure legend, the reader is referred to the Web version of this article.)

5. Conclusion

Overall, the current study identified candidate proteins as well as their associated biological processes and pathways involved in the chronic physiological adaptation of the pearl oyster *P. fucata martensii* following nucleus implantation. During the 30-day experiment, a wide variety of proteins, including a group of immune-related proteins such as E3 ubiquitin-ligase and heat shock proteins, exhibited differential expression at different time points. Moreover, proteins related to GO terms including “translation” and “oxidation-reduction process” and KEGG pathways including “glycolysis/gluconeogenesis” and “pyruvate metabolism” were significantly enriched at multiple sampling points, indicating the crucial roles of these molecular events in the stress response of *P. fucata martensii* to nucleus implantation. In addition, considerable discrepancy between protein expression data and gene transcript abundancy was identified, implying that post-transcriptional gene regulation for the key proteins may represent an important aspect of allograft-induced stress response in the pearl oysters.

Acknowledgement

The current study was funded by the National Natural Science Foundation of China (Grant No. 31472306), Special Fund for Harbor Construction and Fishery Industry Development of Guangdong Province (Grant No. A201608B15), a Start-up Fund from Guangdong Ocean University, and a fund from Natural Science Foundation of Guangdong Province (Gant No. 2018A030310049). The authors are grateful to the reviewers for their constructive suggestions on an earlier version of this manuscript.

Appendix A. Supplementary data

Supplementary data to this article can be found online at https://doi.org/10.1016/j.fsi.2018.11.044.

References

[1] E.L. McGinty, B.S. Evans, J.U.U. Taylor, D.R. Jerry, Xenografts and pearl production in two pearl oyster species, *P. maxima* and *P. margaritifera*: effect on pearl quality and a key to understanding genetic contribution, Aquaculture 302 (3) (2010) 175–181.

[2] P. Kishore, P.C. Southgate, The effect of different culture methods on the quality of round pearls produced by the black-lip pearl oyster *Pinctada margaritifera* (Linnaeus, 1758), Aquaculture 451 (2016) 65–71.

[3] W. Wang, Y. Wu, Q. Lei, H. Liang, Y. Deng, Deep transcriptome profiling sheds light on key players in nucleus implantation induced immune response in the pearl oyster *Pinctada martensii*, Fish Shellfish Immunol. 69 (2017) 67–77.

[4] P. Kishore, P.C. Southgate, A detailed description of pearl-sac development in the black-lip pearl oyster, *Pinctada margaritifera (Linnaeus 1758)*, Aquacult. Res. 47 (7) (2016) 2215–2226.

[5] G. Le Moullac, L. Schuck, S. Chabrier, C. Belliard, P. Lyonnard, F. Broustal, C. Soyez, D. Saulnier, C. Brahmi, C.L. Ky, B. Beliaeff, Influence of temperature and pearl rotation on biomineralization in the pearl oyster, *Pinctada margaritifera*, J. Exp. Biol. 221 (Pt 18) (2018).

[6] M. Shinohara, S. Kinoshita, E. Tang, D. Funabara, M. Kakinuma, K. Maeyama, K. Nagai, M. Awaji, S. Watabe, S. Asakawa, Comparison of two pearl sacs formed in

the same recipient oyster with different genetic background involved in yellow pigmentation in *Pinctada Fucata*, Mar Biotechnol (NY) 20 (5) (2018) 594–602.
[7] T. Takeuchi, T. Kawashima, R. Koyanagi, F. Gyoja, M. Tanaka, T. Ikuta, E. Shoguchi, M. Fujiwara, C. Shinzato, K. Hisata, M. Fujie, T. Usami, K. Nagai, K. Maeyama, K. Okamoto, H. Aoki, T. Ishikawa, T. Masaoka, A. Fujiwara, K. Endo, H. Endo, H. Nagasawa, S. Kinoshita, S. Asakawa, S. Watabe, N. Satoh, Draft genome of the pearl oyster *Pinctada fucata*: a platform for understanding bivalve biology, DNA Res. 19 (2) (2012) 117–130.
[8] X. Zhao, Q. Wang, Y. Jiao, R. Huang, Y. Deng, H. Wang, X. Du, Identification of genes potentially related to biomineralization and immunity by transcriptome analysis of pearl sac in pearl oyster *Pinctada martensii*, Mar. Biotechnol. 14 (6) (2012) 730–739.
[9] J. Wei, B. Liu, S. Fan, B. Zhang, J. Su, D. Yu, Serum immune response of pearl oyster *Pinctada fucata* to xenografts and allografts, Fish Shellfish Immunol. 62 (2017) 303–310.
[10] J. Wei, B. Liu, S. Fan, H. Li, M. Chen, B. Zhang, J. Su, Z. Meng, D. Yu, Differentially expressed immune-related genes in hemocytes of the pearl oyster *Pinctada fucata* against allograft identified by transcriptome analysis, Fish Shellfish Immunol. 62 (2017) 247–256.
[11] W. Zhu, S. Fan, G. Huang, D. Zhang, B. Liu, X. Bi, D. Yu, Highly expressed EGFR in pearl sac may facilitate the pearl formation in the pearl oyster, *Pinctada fucata*, Gene 566 (2) (2015) 201–211.
[12] Y. Li, X. Huang, Y. Guan, Y. Shi, H. Zhang, M. He, DNA methylation is associated with expression level changes of galectin gene in mantle wound healing process of pearl oyster, *Pinctada fucata*, Fish Shellfish Immunol. 45 (2) (2015) 912–918.
[13] J. Li, J. Chen, Y. Zhang, Z. Yu, Expression of allograft inflammatory factor-1 (AIF-1) in response to bacterial challenge and tissue injury in the pearl oyster, *Pinctada martensii*, Fish Shellfish Immunol. 34 (1) (2013) 365–371.
[14] P. Kishore, P.C. Southgate, Development and function of pearl-sacs grown from regenerated mantle graft tissue in the black-lip pearl oyster, *Pinctada margaritifera* (Linnaeus, 1758), Fish Shellfish Immunol. 45 (2) (2015) 567–573.
[15] S.Z. Wu, X.D. Huang, Q. Li, M.X. He, Interleukin-17 in pearl oyster (*Pinctada fucata*): molecular cloning and functional characterization, Fish Shellfish Immunol. 34 (5) (2013) 1050–1056.
[16] H. Chen, X. Diao, H. Wang, H. Zhou, An integrated metabolomic and proteomic study of toxic effects of Benzo[a]pyrene on gills of the pearl oyster *Pinctada martensii*, Ecotoxicol. Environ. Saf. 156 (2018) 330–336.
[17] J. Wei, S. Fan, B. Liu, B. Zhang, J. Su, D. Yu, Transcriptome analysis of the immune reaction of the pearl oyster *Pinctada fucata* to xenograft from *Pinctada maxima*, Fish Shellfish Immunol. 67 (2017) 331–345.
[18] Y. Fu, F. Zhu, L. Liu, S. Lu, Z. Ren, C. Mu, R. Li, W. Song, C. Shi, Y. Ye, C. Wang, iTRAQ-based proteomic analysis identifies proteins involved in limb regeneration of swimming crab *Portunus trituberculatus*, Comp. Biochem. Physiol. Genom. Proteonomics 26 (2018) 10–19.
[19] S. Jin, H. Fu, S. Sun, S. Jiang, Y. Xiong, Y. Gong, H. Qiao, W. Zhang, Y. Wu, iTRAQ-based quantitative proteomic analysis of the androgenic glands of the oriental river prawn, *Macrobrachium nipponense*, during nonreproductive and reproductive seasons, Comp. Biochem. Physiol. Genom. Proteonomics 26 (2018) 50–57.
[20] H. Li, B. Zhang, S. Fan, B. Liu, J. Su, D. Yu, Identification and differential expression of biomineralization genes in the mantle of pearl oyster *Pinctada fucata*, Mar. Biotechnol. 19 (3) (2017) 266–276.
[21] C. Blay, S. Planes, C.L. Ky, Donor and recipient contribution to phenotypic traits and the expression of biomineralisation genes in the pearl oyster model *Pinctada margaritifera*, Sci. Rep. 7 (1) (2017) 2696.
[22] Y. Guan, M. He, H. Wu, Differential mantle transcriptomics and characterization of growth-related genes in the diploid and triploid pearl oyster *Pinctada fucata*, Mar Genomics 33 (2017) 31–38.
[23] H. Zhang, X. Huang, Y. Shi, W. Liu, M. He, Identification and analysis of an MKK4 homologue in response to the nucleus grafting operation and antigens in the pearl oyster, *Pinctada fucata*, Fish Shellfish Immunol. 73 (2018) 279–287.
[24] C. Blay, S. Planes, C.L. Ky, Optimal age of the donor graft tissue in relation to cultured pearl phenotypes in the mollusc, *Pinctada margaritifera*, PLoS One 13 (6) (2018) e0198505.
[25] M.H. Bengtson, C.A.P. Joazeiro, Role of a ribosome-associated E3 ubiquitin ligase in protein quality control, Nature 467 (2010) 470.
[26] R. Rajsbaum, A. Garcia-Sastre, G.A. Versteeg, TRIMmunity: the roles of the TRIM E3-ubiquitin ligase family in innate antiviral immunity, J. Mol. Biol. 426 (6) (2014) 1265–1284.
[27] M. Yang, C. Wang, X. Zhu, S. Tang, L. Shi, X. Cao, T. Chen, E3 ubiquitin ligase CHIP facilitates Toll-like receptor signaling by recruiting and polyubiquitinating Src and atypical PKC{zeta}, J. Exp. Med. 208 (10) (2011) 2099–2112.
[28] G. Meroni, G. Diez-Roux, TRIM/RBCC, a novel class of 'single protein RING finger' E3 ubiquitin ligases, Bioessays 27 (11) (2005) 1147–1157.
[29] F.W. McNab, R. Rajsbaum, J.P. Stoye, A. O'Garra, Tripartite-motif proteins and innate immune regulation, Curr. Opin. Immunol. 23 (1) (2011) 46–56.
[30] T. Kawai, S. Akira, Regulation of innate immune signalling pathways by the tripartite motif (TRIM) family proteins, EMBO Mol. Med. 3 (9) (2011) 513–527.
[31] G.A. Versteeg, R. Rajsbaum, M.T. Sanchez-Aparicio, A.M. Maestre, J. Valdiviezo, M. Shi, K.S. Inn, A. Fernandez-Sesma, J. Jung, A. Garcia-Sastre, The E3-ligase TRIM family of proteins regulates signaling pathways triggered by innate immune pattern-recognition receptors, Immunity 38 (2) (2013) 384–398.
[32] P.D. Uchil, B.D. Quinlan, W.T. Chan, J.M. Luna, W. Mothes, TRIM E3 ligases interfere with early and late stages of the retroviral life cycle, PLoS Pathog. 4 (2) (2008) e16.
[33] P. Jacob, H. Hirt, A. Bendahmane, The heat-shock protein/chaperone network and multiple stress resistance, Plant Biotechnol. J 15 (4) (2017) 405–414.
[34] A. Jolesch, K. Elmer, H. Bendz, R.D. Issels, E. Noessner, Hsp70, a messenger from hyperthermia for the immune system, Eur. J. Cell Biol. 91 (1) (2012) 48–52.
[35] H. Cwiklinska, M.P. Mycko, B. Szymanska, M. Matysiak, K.W. Selmaj, Aberrant stress-induced Hsp70 expression in immune cells in multiple sclerosis, J. Neurosci. Res. 88 (14) (2010) 3102–3110.
[36] M.P. Mycko, H. Cwiklinska, A. Walczak, C. Libert, C.S. Raine, K.W. Selmaj, A heat shock protein gene (Hsp70.1) is critically involved in the generation of the immune response to myelin antigen, Eur. J. Immunol. 38 (7) (2008) 1999–2013.
[37] J.R. Bradley, J.S. Pober, Tumor necrosis factor receptor-associated factors (TRAFs), Oncogene 20 (44) (2001) 6482 6291.
[38] R.H. Arch, R.W. Gedrich, C.B. Thompson, Tumor necrosis factor receptor-associated factors (TRAFs)–a family of adapter proteins that regulates life and death, Genes Dev. 12 (18) (1998) 2821–2830.
[39] N.K. Lee, S.Y. Lee, Modulation of life and death by the tumor necrosis factor receptor-associated factors (TRAFs), J. Biochem. Mol. Biol. 35 (1) (2002) 61–66.
[40] W.W. Sun, X.X. Zhang, W.S. Wan, S.Q. Wang, X.B. Wen, H.P. Zheng, Y.L. Zhang, S.K. Li, Tumor necrosis factor receptor-associated factor 6 (TRAF6) participates in anti-lipopolysaccharide factors (ALFs) gene expression in mud crab, Dev. Comp. Immunol. 67 (2017) 361–376.
[41] N.L. Malinin, M.P. Boldin, A.V. Kovalenko, D. Wallach, MAP3K-related kinase involved in NF-kappaB induction by TNF, CD95 and IL-1, Nature 385 (6616) (1997) 540–544.
[42] X. Li, Y. Yang, J.D. Ashwell, TNF-RII and c-IAP1 mediate ubiquitination and degradation of TRAF2, Nature 416 (6878) (2002) 345–347.
[43] J.A. Weiner, Protocadherins and other atypical cadherins, Semin. Cell Dev. Biol. 69 (2017) 69.
[44] J.A. Weiner, J.D. Jontes, Protocadherins, not prototypical: a complex tale of their interactions, expression, and functions, Front. Mol. Neurosci. 6 (2013) 4.
[45] H. Morishita, T. Yagi, Protocadherin family: diversity, structure, and function, Curr. Opin. Cell Biol. 19 (5) (2007) 584–592.
[46] P. Zhang, H. Wang, J. Wang, Q. Liu, Y. Wang, F. Feng, L. Shi, Association between protocadherin 8 promoter hypermethylation and the pathological status of prostate cancer, Oncol Lett 14 (2) (2017) 1657–1664.
[47] N. Inoue, R. Ishibashi, T. Ishikawa, T. Atsumi, H. Aoki, A. Komaru, Gene expression patterns in the outer mantle epithelial cells associated with pearl sac formation, Mar. Biotechnol. 13 (3) (2011) 474–483.
[48] D.B. Jones, D.R. Jerry, S. Foret, D.A. Konovalov, K.R. Zenger, Genome-wide SNP validation and mantle tissue transcriptome analysis in the silver-lipped pearl oyster, *Pinctada maxima*, Mar. Biotechnol. 15 (6) (2013) 647–658.
[49] Z. Yan, Z. Fang, Z. Ma, J. Deng, S. Li, L. Xie, R. Zhang, Biomineralization: functions of calmodulin-like protein in the shell formation of pearl oyster, Biochim. Biophys. Acta 1770 (9) (2007) 1338–1344.
[50] D. Becker, Y. Reydelet, J.A. Lopez, C. Jackson, J.K. Colbourne, S. Hawat, M. Hippler, B. Zeis, R.J. Paul, The transcriptomic and proteomic responses of *Daphnia pulex* to changes in temperature and food supply comprise environment-specific and clone-specific elements, BMC Genomics 19 (1) (2018) 376.
[51] H. Gan, T. Cai, X. Lin, Y. Wu, X. Wang, F. Yang, C. Han, Integrative proteomic and transcriptomic analyses reveal multiple post-transcriptional regulatory mechanisms of mouse spermatogenesis, Mol. Cell. Proteomics 12 (5) (2013) 1144–1157.
[52] D. Fu, J. Chen, Y. Zhang, Z. Yu, Cloning and expression of a heat shock protein (HSP) 90 gene in the haemocytes of *Crassostrea hongkongensis* under osmotic stress and bacterial challenge, Fish Shellfish Immunol. 31 (1) (2011) 118–125.